

Crystal and Molecular Structure of Rubidium Peroxodicarbonate $\text{Rb}_2[\text{C}_2\text{O}_6]$

Robert E. Dinnebier, Sascha Vensky, and Martin Jansen*^[a]

Abstract: We report the crystal structure of rubidium peroxodicarbonate, which was synthesized by electrocrystallization at $T=257\text{ K}$, from laboratory X-ray powder diffraction data. The compound crystallizes in the monoclinic space group $P2_1/c$ with four formula units per unit cell and cell parameters of $a=7.9129(1)$, $b=10.5117(1)$, $c=$

$7.5559(1)\text{ \AA}$, $\beta=102.001(1)^\circ$, and $V=614.75(1)\text{ \AA}^3$. The packing can be considered as a strongly distorted CsCl type

Keywords: electrocrystallization • peroxodicarbonate • simulated annealing • solid-state structure • X-ray powder diffraction

of structure. The conformation of the peroxodicarbonate anion was found to be planar (C_{2h} symmetry), in contrast to the staggered conformation of the peroxodicarbonate anion in the respective potassium peroxodicarbonate. The different conformation is attributed to packing effects.

Introduction

The derivatives of H_2O_2 , organic as well as inorganic, constitute an extended family of industrial chemicals^[1] that find widespread applications as initiators in polymerization, as selective oxidants in chemical synthesis, as non-selective oxidants for waste water regeneration, as bleaching agents, or as disinfectants.^[2–6] At the same time, they have always attracted significant academic interest since the basic features of the respective central O–O bond, length and dihedral angle, are determined by an intricate interplay of various interactions. These range from crystal packing effects, Pauli and Coulomb repulsions between the attached groups, and antibonding π -orbital interactions, whereby the latter, crucially depend on the electronegativity of the substituents. Accordingly, the dihedral angles across the O–O bonds in peroxides vary over the wide range from $86,7^\circ$ to 180° . Typically, values around 90° are found for H_2O_2 itself, and for peroxides with small organic groups. Bulky organic substituents lead to dihedral angles approaching 180° and also all structures of peroxodioxo anions known at the beginning of our work mainly showed torsion angles of 180° (Table 1). Thus, it came as a surprise when we observed a dihedral angle as small as 93° for potassium peroxodicarbonate.^[7] To get closer insights into the reasons behind this feature we have investigated the related compound $\text{Rb}_2[\text{C}_2\text{O}_6]$.

Rubidium peroxodicarbonate^[27] as well as the corresponding potassium compound^[27, 28] were first described in the literature at the end of the 19th century. They were synthesized by anodic oxidation, the technique still used today. The constitution of the peroxodicarbonate ion was claimed as an anion built of two carbonate groups linked by a peroxy group.^[27, 29–32] After this discovery some reinvestigation took place in the 1960s, which focused on work with the more stable potassium peroxodicarbonate.^[33–36] X-ray powder diffraction investigations of that time failed to find the correct unit cells and X-ray densities for rubidium and potassium peroxodicarbonate.^[37, 34, 36] Early quantum-chemical calculations^[38] suggested a staggered conformation (C_2 symmetry) for the peroxodicarbonate anion, while investigations using IR and Raman spectroscopy^[34, 39, 40] indicated a planar conformation (C_{2h} symmetry), which could not be verified for potassium peroxodicarbonate (C_2 symmetry).^[7]

Results and Discussion

The peroxodicarbonate ion (Figure 1 top) in rubidium peroxodicarbonate consists of two carbonate groups connected through two of its oxygen atoms to form a peroxy group. The molecular symmetry was found to be C_{2h} within the limits of experimental error. The carbon atoms are surrounded by oxygen atoms in a largely trigonal-planar arrangement. The bond lengths between the carbon and the peroxy-oxygen atoms is increased by up to 10% compared to the bond lengths between carbon and the terminal oxygen atoms. In general, the intramolecular bond lengths and angles of the carbonate group are within the range typically found for this class of molecules (Table 1). The deviations from planarity for

[a] Prof. Dr. M. Jansen, Priv.-Doz. Dr. R. E. Dinnebier, Dipl.-Chem. S. Vensky
Max-Planck-Institute for Solid State Research
Heisenbergstrasse 1, 70569 Stuttgart (Germany)
Fax: (+49) 711-689-1502
E-mail: m.jansen@fkf.mpg.de

Table 1. Selected bond lengths [\AA] and torsion angles [$^\circ$] for $\text{Rb}_2[\text{C}_2\text{O}_6]$ and related molecules.

Substance	Ref.	$d(\text{O}-\text{O})$	$d(\text{A}-\text{O})$	$d(\text{C}-\text{O})$	$d(\text{C}-\text{O}_\text{O})$	C-O-O-C
$\text{Rb}_2[\text{C}_2\text{O}_6]^{\text{[a]}}$		1.47(2)	2.70(2)–3.44(1)	1.22(2)–1.26(2)	1.33(2)	175(1)
$\text{K}_2[\text{C}_2\text{O}_6]^{\text{[a]}}$	[7]	1.47(1)	2.63(1)–2.90(1)	1.26(2)–1.29(2)	1.31(1)	93(1)
$\text{KHCO}_4 \cdot \text{H}_2\text{O}_2$	[8]	1.46	2.75–2.83	1.23–1.25	1.38	101 _{COOH}
$\text{RbHCO}_4 \cdot 0.5\text{H}_2\text{O}_2$	[9]	1.46	2.89–3.34	–	–	–
H_2O_2	[10]	1.46	–	–	–	93 _{HOOH}
K_2O_2	[11]	1.54	2.68–2.71	–	–	–
Rb_2O_2	[12]	1.51	2.84–2.85	–	–	–
K_2CO_3	[13]	–	2.64–3.14	1.27–1.29	–	–
Rb_2CO_3	[14]	–	2.59–3.24	1.29–1.30	–	–
$\text{Rb}_2\text{CO}_3 \cdot 1.5\text{H}_2\text{O}$	[15]	–	2.87–3.37	1.27–1.29	–	–
$\text{Rb}_4(\text{HCO}_3)_2(\text{CO}_3) \cdot \text{H}_2\text{O}$	[16]	–	2.88–3.31	1.25–1.34	–	–
$\alpha\text{-Rb}_2[\text{C}_2\text{O}_6]$	[17]	–	2.82–3.58	1.19–1.25	–	–
$\beta\text{-Rb}_2[\text{C}_2\text{O}_6]$	[17]	–	2.96–3.05	1.19–1.24	–	–
$\text{K}_2[\text{S}_2\text{O}_8]$	[18]	1.50	2.75–3.09	–	–	180
$(\text{NH}_4)_4[\text{P}_2\text{O}_8] \cdot 2\text{H}_2\text{O}$	[19]	1.50	–	–	–	180
$(\text{H}_{11}\text{C}_6)_2\text{C}_2\text{O}_6$	[20]	1.43	–	1.18–1.32	1.38–1.39	90
$(\text{HO}_2\text{C}-\text{C}_2\text{H}_4-\text{CO}_2)_2$	[21]	1.45	–	1.18–1.19	1.38	89
$(\text{H}_5\text{C}_6\text{CO}_2)_2$	[22]	1.43	–	1.17–1.20	1.36–1.39	91
$((\text{H}_3\text{C}-\text{O}-\text{C}_6\text{H}_4)\text{CO}_2)_2$	[23]	1.46	–	1.18	1.40	87
$((\text{H}_5\text{C}_6)_3\text{CCH}_2)\text{CO}_2)_2$	[24]	1.48	–	1.18	1.28	180
$(\text{H}_3\text{C}_3\text{Si})_2\text{O}_2$	[25]	1.50	–	–	–	180

[a] The given esds are Rietveld statistical estimates and should be multiplied by a factor of up to six according to reference^[26].

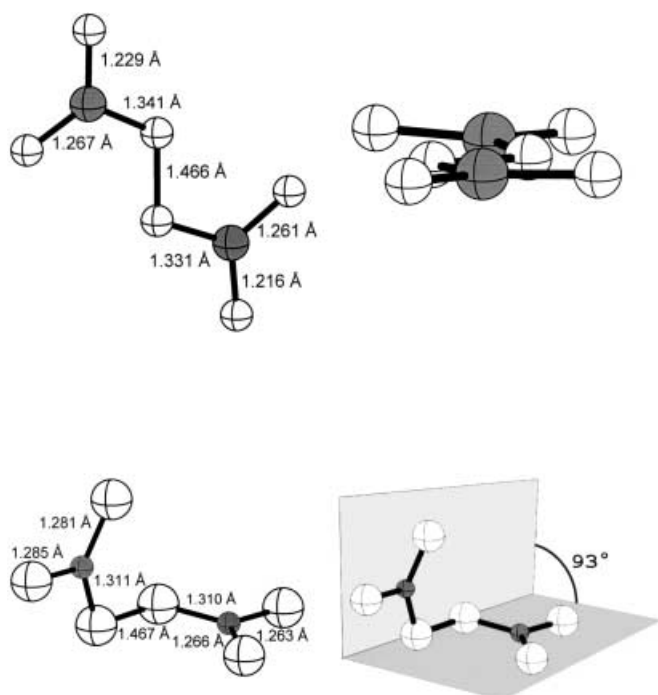


Figure 1. Conformations of the peroxodicarbonate anion in $\text{Rb}_2[\text{C}_2\text{O}_6]$ at $T = 200\text{ K}$ (top) and in $\text{K}_2[\text{C}_2\text{O}_6]$ at $T = 150\text{ K}$ (bottom).

the carbonate groups including the second peroxy-oxygen atom are below the level of accuracy of the measurement. The bond length of $1.47(2)\text{ \AA}$ between the oxygen atoms of the peroxy group is virtually identical for peroxy groups in related compounds, such as potassium peroxodicarbonate,^[7] potassium hydrogen peroxocarbonate perhydrate,^[8] and rubidium hydrogen peroxocarbonate semiperhydrate.^[9] The dihedral angle C-O-O-C within the peroxodicarbonate anion is almost 180° ($175(1)^\circ$) for $\text{Rb}_2[\text{C}_2\text{O}_6]$ (Table 1).

The two crystallographically independent rubidium cations ($\text{Rb}(1)/\text{Rb}(2)$) are irregularly coordinated to eight ($\text{Rb}(2)\text{O}_8$) and ten oxygen atoms ($\text{Rb}(1)\text{O}_{10}$), respectively (Figure 2). The distances between the rubidium atoms and the oxygen

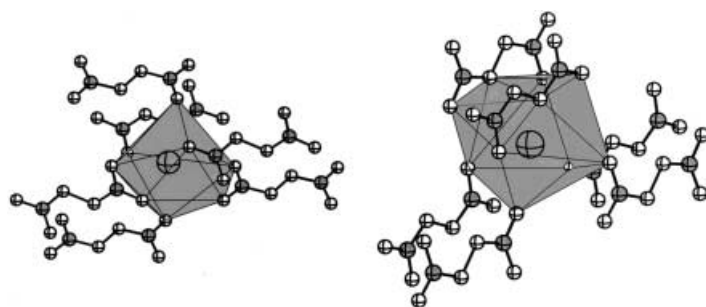


Figure 2. Representation of the two crystallographically distinct $\text{Rb}(2)\text{O}_8$ (left) and $\text{Rb}(1)\text{O}_{10}$ (right) coordination polyhedra and coordinated $[\text{C}_2\text{O}_6]^{2-}$ ions in rubidium peroxodicarbonate at $T = 200\text{ K}$.

atoms range between $2.70(2)$ and $3.44(1)\text{ \AA}$, and are thus comparable to that in related compounds (Table 1). The cut-off radius for the Rb–O distances has been selected by calculating the effective coordination number (ECoN)^[41] and the mean fictive ionic radii (MeFIR)^[41] by using the program MAPLE.^[42] Both polyhedra are connected to six different peroxodicarbonate anions (Figure 2). The $\text{Rb}(2)\text{O}_8$ polyhedron shares two edges and four corners with carbonate subgroups, whereas the $\text{Rb}(1)\text{O}_{10}$ polyhedron shares two edges and six corners with carbonate subgroups. The two additional rubidium oxygen coordinations in the case of $\text{Rb}(1)\text{O}_{10}$ are achieved by coordinating simultaneously both carbonate subgroups of two different peroxodicarbonate anions to the $\text{Rb}(1)\text{O}_{10}$ polyhedron. It should be noted that no edge of the rubidium–oxygen polyhedra is equivalent to a peroxy bridge. The two rubidium–oxygen polyhedra are

alternately connected through triangular faces to form infinite chains. Parallel chains form infinite layers, where $\text{Rb}(2)\text{O}_8$ polyhedra are connected through rectangular faces on both sides, and neighboring $\text{Rb}(1)\text{O}_{10}$ polyhedra share common edges on both sides. Consecutive layers are connected through common edges and triangular faces and interconnected by peroxodicarbonate anions, completing the three-dimensional framework structure (Figure 3 right). For a better

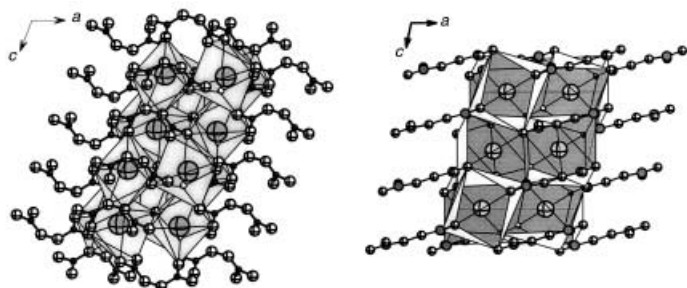


Figure 3. Crystal structures of potassium peroxodicarbonate at $T=150$ K (left) and rubidium peroxodicarbonate at $T=200$ K (right) viewed along the b axis.

understanding, the carbonate groups may be substituted by their center of gravity (carbon atoms), accordingly the crystal structure of $\text{Rb}_2[\text{C}_2\text{O}_6]$ can be viewed as a strongly distorted CsCl structure (Figure 4 left).

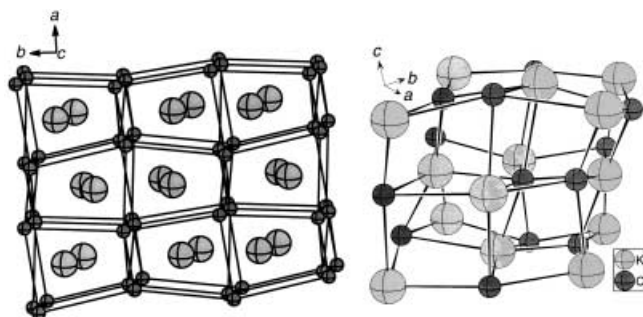


Figure 4. Packing schemes of potassium peroxodicarbonate at $T=150$ K (right) and rubidium peroxodicarbonate at $T=200$ K (left). For $\text{K}_2[\text{C}_2\text{O}_6]$ in a view perpendicular to the plane spanned by the c axis and the median of a and b axes. For $\text{Rb}_2[\text{C}_2\text{O}_6]$ in a view along the c axis. The structural relationships to the NaCl type of structure for the potassium compound and the CsCl type of structure for the rubidium compound are clearly visible.

Although, $\text{K}_2[\text{C}_2\text{O}_6]$ and $\text{Rb}_2[\text{C}_2\text{O}_6]$ have an identical space group, an identical number of formula units, and similar lattice parameters (Table 2), the crystal structures are quite different. This can be attributed to the different size and polarizability of the cations. Fully in line with the general trends in crystal chemistry of alkali metals, rubidium peroxodicarbonate can be reduced to a CsCl-type arrangement (Figure 4 left), while the packing of potassium peroxodicarbonate can be reduced to a NaCl-type configuration (Figure 4 right).^[7]

With respect to the conformations of the peroxodicarbonate anions, the crystal structures of $\text{K}_2[\text{C}_2\text{O}_6]$ and $\text{Rb}_2[\text{C}_2\text{O}_6]$ feature a prominent and unexpected contrast. While the

Table 2. Crystallographic data for $\text{Rb}_2[\text{C}_2\text{O}_6]$ in comparison with $\text{K}_2[\text{C}_2\text{O}_6]$.^[7]

	$\text{Rb}_2[\text{C}_2\text{O}_6]$	$\text{K}_2[\text{C}_2\text{O}_6]$
temperature [K]	200	150
formula weight [g mol^{-1}]	290.954	198.215
space group; no.	$P2_1/c$; 14	$P2_1/c$; 14
Z	4	4
a [Å]	7.9129(1)	8.3805(1)
b [Å]	10.5117(1)	10.7641(2)
c [Å]	7.5559(1)	7.1167(1)
β [°]	102.001(1)	111.24(0)
V [Å ³]	614.75(1)	598.4(2)
ρ_{calcd} [g cm^{-3}]	3.144	2.200
λ [Å]	1.54059	1.12074(2)
capillary diameter [mm]	0.2	0.7
absorption [cm^{-1}]	193.66	55.04

dihedral angle across the O–O bond is 93° (Figure 1 bottom) in $\text{K}_2[\text{C}_2\text{O}_6]$,^[7] it is 175° in the rubidium compound, resulting in an almost planar anion (Figure 1 top). In principle, both geometries can be justified in a first approximation based on arguments related to intramolecular interactions, only. Assuming the bridging oxygen atoms to be sp^2 hybridized would lead to a p_z orbital oriented perpendicular to the CO_3 plane. This would result in a strong π repulsion of the occupied p_z orbital in a planar geometry, thus favouring conformations with C–O–O–C around 90° , as has been found for $\text{K}_2[\text{C}_2\text{O}_6]$. On the other hand, sp^3 hybridization of the bridging oxygen atoms would lead to dihedral angles approaching 180° which in addition would minimize the Coulomb repulsion of the CO_3 units. Unfortunately, for each of these two scenarios the expected responses of bond lengths and angles within the anion are below the margin of error of the structural data as determined experimentally. However, it is obvious that the packing requirements play a decisive role in fixing the torsional O–O angle to one of the local minima mentioned.

This feature is similar to what has been observed for the oxalate anion in alkali oxalates.^[17] Here the oxalate anion in potassium oxalate is planar, while in cesium oxalate it is staggered with a dihedral angle of 99° , and for rubidium oxalate both conformations are observed, which at room temperature even can coexist.^[17]

Experimental Section

$\text{Rb}_2[\text{C}_2\text{O}_6]$ was synthesized by anodic oxidation of a saturated aqueous solution of rubidium carbonate (p.a., Merck) at $T=257$ K. The electrocrystallization was carried out under galvanostatic conditions ($I=250$ mA, $U \geq 16$ V) with a potentiostat (EG&G Princeton Applied Research, Type 363). A Pt wire ($\varnothing=0.5$ mm, $l=40$ mm) was used as an anode, a Pt mesh ($\varnothing_{\text{Zyl}}=40$ mm, $h=50$ mm, 20 mesh) as a cathode. The anodic part was separated by a glassy membrane. Rubidium peroxodicarbonate, obtained as a microcrystalline, colorless to light blue powder, was filtered and washed with ethanol and diethyl ether. $\text{Rb}_2[\text{C}_2\text{O}_6]$ is very hygroscopic^[27] and decomposes even when stored at 247 K. According to the results of thermal analysis (DTA/TG/MS; Netzsch STA 429; 293–1273 K; 10 K min^{-1}), $\text{Rb}_2[\text{C}_2\text{O}_6]$ starts decomposing at 424 K ($\text{K}_2[\text{C}_2\text{O}_6]$ at 394 K) by generation of oxygen and carbon dioxide.

X-ray powder diffraction data of rubidium peroxodicarbonate were collected with a Stoe Stadi-P transmission diffractometer (primary beam Johann-type Ge monochromator for $\text{Cu}_{\text{K}\alpha 1}$ radiation, linear PSD) in 2θ steps of 0.01° from 10.0° to 100.0° at a temperature of $T=200$ K for 65 h

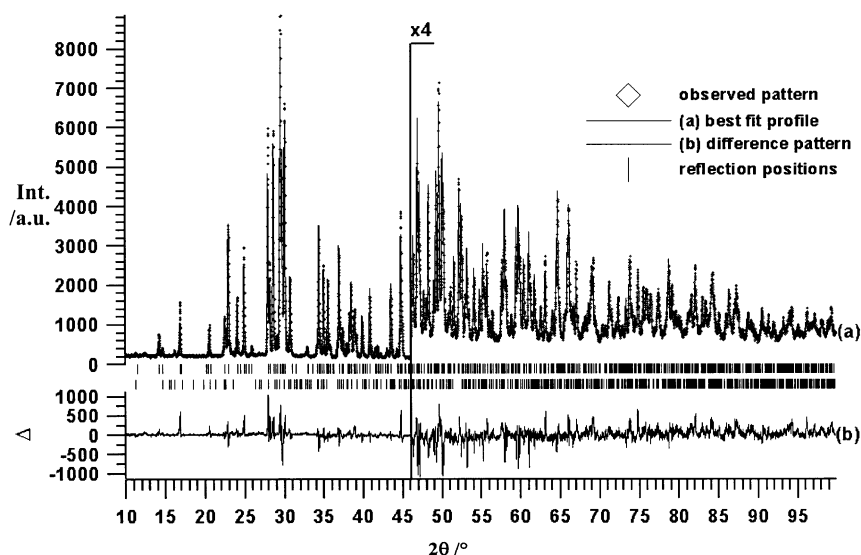


Figure 5. Scattered X-ray intensity for rubidium peroxodicarbonate at $T=200$ K as a function of diffraction angle 2θ . Shown are the observed pattern (diamonds), the best Rietveld-fit profile in $P2_1/c$, the enlarged difference curve between observed and calculated profile (below in an additional window), and the reflection markers (vertical bars). The wavelength was $\lambda = 1.54059$ Å. Agreement factors for 628 reflections and 50 variables are $R_p = 0.084$, $R_{wp} = 0.107$, $R_F = 0.069$, and $R_F^2 = 0.108$, as defined in GSAS.^[47] The higher angle part starting at $2\theta = 46^\circ$ is enlarged by a factor of 4. $\text{Rb}_4(\text{HCO}_3)_2(\text{CO}_3) \cdot \text{H}_2\text{O}^{[16]}$ was included as a second phase.

with the sample sealed in a glass capillary of 0.2 mm diameter (Hilgenberg, glass No. 50) (Figure 5). Weak reflections corresponding to small traces of $\text{Rb}_4(\text{HCO}_3)_2(\text{CO}_3) \cdot \text{H}_2\text{O}^{[16]}$ as an additional phase were observed in the scan. Further experimental details are given in Table 2.

Data reduction was performed by using the GUFU program.^[43] Indexing with ITO^[44] led to a primitive orthorhombic unit cell with lattice parameters given in Table 2. The number of formula units per unit cell could be determined to be $Z=4$ from packing considerations. The extinctions found in the powder patterns indicated $P2_1/c$ as the most probable space group, which could later be confirmed by Rietveld refinements.^[45] The peak profiles and precise lattice parameters were determined by LeBail-type fits^[46] using the programs GSAS^[47] and FULLPROF.^[48, 49] The background was modeled manually by using GUFU. The peak profile was described by a pseudo-Voigt function in combination with a special function that accounts for the asymmetry due to axial divergence.^[50–52]

The crystal structure of rubidium peroxodicarbonate was subsequently solved by using the DASH structure solution package.^[53] The measured powder patterns were subjected to a Pawley refinement^[54] in the space group $P2_1/c$ to extract correlated integrated intensities from the pattern. Good fits to the data were obtained. An internal coordinate description of the peroxodicarbonate moiety (Figure 1 top) was constructed by using bond lengths, angles, and torsion angles from the corresponding potassium compound, $\text{K}_2[\text{C}_2\text{O}_6]$.^[7] The torsion angles between the two carbonate groups could not be assigned precise values in advance, and thus they were treated as variables for refinement in the simulated annealing procedure. The position of two crystallographically independent rubidium cations as well as the position, orientation, and conformation of the peroxodicarbonate anions in the unit cell were postulated, and the level of agreement between the trial structure and the experimental diffraction data quantified by Equation (1).

$$\chi^2 = \sum_h \sum_k [(I_h - c |F_h|^2)(V^{-1})_{hk} (I_k - c |F_k|^2)] \quad (1)$$

Here I_h and I_k are Lorentz-polarization corrected, extracted integrated intensities from the Pawley refinement of the diffraction data, V_{hk} is the covariance matrix from the Pawley refinement, c is a scale factor, and $|F_h|$ and $|F_k|$ are the structure factor magnitudes calculated from the trial structure. The trial structure was subjected to global optimization with DASH^[53] where the torsion angle between the carbonate groups and the

bond length between the oxygen atoms were the only internal degrees of freedom. The external degrees of freedom consisted of the fractional coordinates describing the positions of the rubidium cations and the peroxodicarbonate ions, and four quaternions^[55] describing the orientation of the anion. The structure giving the best fit to the data was validated by Rietveld refinement of the fractional coordinates obtained at the end of the simulated annealing run.

Rietveld refinements were performed on the powder pattern of $\text{Rb}_2[\text{C}_2\text{O}_6]$ by using the program package GSAS (Figure 5). The background was modeled manually by using GUFU. $\text{Rb}_4(\text{HCO}_3)_2(\text{CO}_3) \cdot \text{H}_2\text{O}^{[16]}$ was included in the refinement as an additional phase. The peak profile was described by a pseudo-Voigt function, in combination with a special function that accounted for the asymmetry due to axial divergence.^[50, 51] Due to the excellent reflection to parameter ratio, only weak soft constraints were necessary to stabilize the refinements. Agreement factors (R values) are listed in Figure 5, the coordinates are given in Table 3, and a selection of intra- and intermolecular distances and torsion angles is given in Table 1.

Further details of the crystal structure investigation can be obtained from the Fachinformationszentrum Karlsruhe, 76344 Eggenstein-Leopoldshafen, Germany (Fax: (+49) 7247-808-666; e-mail: crysdata@fiz.karlsruhe.de) on quoting the depositary number CSD-412971.

Table 3. Positional parameters and temperature factors for $\text{Rb}_2[\text{C}_2\text{O}_6]$ at $T=200$ K. An overall temperature factor for the peroxodicarbonate moiety was used.

Atom	x	y	z	U_i/U_e [Å ²]
Rb1	0.2454(8)	0.0120(1)	0.5071(8)	5.89(6)
Rb2	0.2498(9)	0.4126(1)	0.497(1)	5.71(6)
O3	0.825(2)	0.291(2)	0.2272(4)	4.47(11)
O4	0.695(2)	0.207(2)	0.2802(4)	4.47(11)
C5	0.561(2)	0.275(1)	0.3063(4)	4.47(11)
O6	0.555(1)	0.394(1)	0.2844(7)	4.47(11)
O7	0.447(2)	0.214(1)	0.3518(5)	4.47(11)
C8	0.962(2)	0.233(1)	0.1843(3)	4.47(11)
O9	1.069(2)	0.304(1)	0.1395(5)	4.47(11)
O10	0.978(2)	0.113(1)	0.1892(7)	4.47(11)

Acknowledgements

Special thanks goes to Sanela Kevric (MPI-FKF at Stuttgart) for her support in sample preparation and to Christian Oberndorfer (MPI-FKF at Stuttgart) for the thermal analysis. Financial support by the Deutsche Forschungsgemeinschaft (DFG), the Bundesministerium für Bildung und Forschung (BMBF), and the Fonds der Chemischen Industrie (FCI) is gratefully acknowledged.

- [1] F. Beer, G. Düsing, H. Pistor, *Chemiker-Zeitung* **1975**, *99*, 120–125.
- [2] J. Muzart, *Synthesis* **1995**, 1325–1347.
- [3] A. McKillop, W. R. Sanderson, *Tetrahedron* **1995**, *51*, 6145–6166.
- [4] R. Ohura, A. Katayama, T. Takagishi, *Text. Res. J.* **1991**, *61*, 242–246.
- [5] J. Tonilelli, *Tenside Deterg.* **1978**, *15*, 252–258.
- [6] G. Jakobi, A. Löhr, M. J. Schwuger, D. Jung, W. Fischer, C. Gloxhuber in *Ullmanns Encyklopädie der technischen Chemie, Vol. 24, Ch. Waschmittel* (Eds. E. Bartholomé, E. Biekert, H. Hellmann, H. Ley, W. M. Weigert, E. Weise), VCH, Weinheim, **1983**, pp. 63–160.

- [7] R. E. Dinnebier, S. Vensky, P. W. Stephens, M. Jansen, *Angew. Chem.* **2002**, *114*, 2002–2004; *Angew. Chem. Int. Ed.* **2002**, *41*, 1922–1924.
- [8] A. Adam, M. Mehta, *Angew. Chem.* **1998**, *110*, 1457–1459; *Angew. Chem. Int. Ed.* **1998**, *37*, 1387–1388.
- [9] A. Adam, M. Mehta, *Z. Kristallogr.* **1998**, *Supplement Issue 15*, 46. This is a conference abstract with no given atomic parameters.
- [10] J.-M. Savariault, M. S. Lehmann, *J. Am. Chem. Soc.* **1980**, *102*, 1298–1303.
- [11] T. Bremm, M. Jansen, *Z. Anorg. Allg. Chem.* **1992**, *610*, 64–66.
- [12] H. Foeppel, *Z. Anorg. Allg. Chem.* **1957**, *291*, 12–50.
- [13] Y. Idemoto, J. W. jr. Richardson, N. Koura, S. Kohara, C.-K. Loong, *J. Phys. Chem. Solids* **1998**, *59*, 363–376.
- [14] H. Ehrhardt, H. Schweer, H. Seidel, *Z. Anorg. Allg. Chem.* **1980**, *462*, 185–198.
- [15] V. Cirpus, J. Wittrock, A. Adam, *Z. Anorg. Allg. Chem.* **2001**, *627*, 533–538.
- [16] V. Cirpus, A. Adam, *Z. Anorg. Allg. Chem.* **1995**, *621*, 1197–1204.
- [17] R. E. Dinnebier, S. Vensky, M. Panthöfer, M. Jansen, *Inorg. Chem.* **2003**, *42*, 1499–1507.
- [18] D. Y. Naumov, A. V. Virovets, N. V. Podberezskaya, P. B. Novikov, A. A. Politov, *J. Struct. Chem.* **1997**, *38*, 772–778.
- [19] W. P. Griffith, R. D. Powell, A. C. Skapski, *Polyhedron* **1988**, *7*, 1305–1310.
- [20] A. Y. Kosnikov, V. L. Antonovskiy, S. V. Lindeman, Y. T. Struchkov, I. P. Zyatkov, *Kristallografiya* **1988**, *33*, 875–877.
- [21] S. V. Lindeman, V. E. Shklover, Y. T. Struchkov, E. K. Starostin, G. I. Nikishin, *Bull. Acad. Sci. USSR Chem. Sci.* **1983**, *32*, 2460–2465.
- [22] J. M. McBride, M. W. Vary, *Tetrahedron* **1982**, *38*, 765–775.
- [23] A. Y. Kosnikov, V. L. Antonovskii, S. V. Lindeman, Y. T. Struchkov, I. P. Zyat'kov, G. A. Pitsevich, V. I. Gogolinskii, *Bull. Acad. Sci. USSR Chem. Sci.* **1985**, *34*, 855–857.
- [24] D. W. Walter, J. M. McBride, *J. Am. Chem. Soc.* **1981**, *103*, 7074–7084.
- [25] D. Königstein, M. Jansen, *Monatsh. Chem.* **1996**, *127*, 1221–1227.
- [26] R. J. Hill, L. M. D. Cranswick, *J. Appl. Crystallogr.* **1994**, *27*, 802–844.
- [27] E. J. Constam, A. von Hansen, *Z. Elektrochem.* **1896**, *3*, 137–144.
- [28] A. von Hansen, *Z. Elektrochem.* **1896**, *3*, 445–448.
- [29] F. Salzer, *Z. Elektrochem.* **1902**, *8*, 893–903.
- [30] E. H. Riesenfeld, B. Reinhold, *Ber. Dtsch. Chem. Ges.* **1909**, *42*, 4377–4383.
- [31] E. H. Riesenfeld, W. Mau, *Ber. Dtsch. Chem. Ges.* **1911**, *44*, 3595–3605.
- [32] J. R. Partington, A. H. Fathallah, *J. Chem. Soc.* **1950**, 1934–1943.
- [33] A. Kh. Mel'nikov, T. P. Firsova, A. N. Molodkina, *Russ. J. Inorg. Chem.* **1962**, *7*, 637–640.
- [34] G. S. Karetnikov, M. F. Sorokina, *Russ. J. Phys. Chem.* **1965**, *39*, 187–189.
- [35] T. P. Firsova, E. Ya. Filatov, *Russ. J. Phys. Chem.* **1968**, *42*, 952–954.
- [36] V. I. Sokol, V. M. Bakulina, E. Ya. Filatov, T. P. Firsova, *Russ. J. Inorg. Chem.* **1968**, *13*, 1211–1212.
- [37] T. P. Firsova, E. Ya. Filatov, V. M. Bakulina, A. N. Zimina, *Russ. J. Inorg. Chem.* **1971**, *16*, 1241–1243.
- [38] C. Glidewell, *J. Mol. Struct.* **1980**, *67*, 35–44.
- [39] P. A. Giguère, D. Lemaire, *Can. J. Chem.* **1972**, *50*, 1472–1477.
- [40] D. P. Jones, W. P. Griffith, *J. Chem. Soc. Dalton Trans.* **1980**, 2526–2532.
- [41] R. Hoppe, *Z. Kristallogr.* **1979**, *150*, 23–52.
- [42] R. Hübenthal, **1991**, MAPLE Vers. 4.0, Dissertation, University of Giessen.
- [43] R. E. Dinnebier, L. Finger, *Z. Krist.* **1998**, *Supplement Issue 15*, 148.
- [44] J. W. Visser, *J. Appl. Crystallogr.* **1969**, *2*, 89–95.
- [45] H. M. Rietveld, *J. Appl. Crystallogr.* **1969**, *2*, 65–71.
- [46] A. Le Bail, H. Duroy, J. L. Fourquet, *Mater. Res. Bull.* **1988**, *23*, 447–452.
- [47] A. C. Larson, R. B. von Dreele, GSAS, General Structure Analysis System, Los Alamos National Laboratory Report LAUR 86–748, Los Alamos National Laboratory, Los Alamos, NM (USA), **2002**.
- [48] J. Rodriguez-Carvajal, *Abstracts of the Satellite Meeting on Powder Diffraction of the XV Congress of the IUCr*, IUCr, Toulouse, **1990**, p. 127.
- [49] J. Rodriguez-Carvajal, Fullprof.2k, version 1.9c, Program for Rietveld Refinement and Pattern Matching Analysis, Laboratoire Leon Brillouin, Gif-sur-Yvette (France), **2001**.
- [50] P. Thompson, D. E. Cox, J. B. Hastings, *J. Appl. Crystallogr.* **1987**, *20*, 79–83.
- [51] L. W. Finger, D. E. Cox, A. P. Jephcoat, *J. Appl. Crystallogr.* **1994**, *27*, 892–900.
- [52] P. W. Stephens, *J. Appl. Crystallogr.* **1994**, *27*, 281–289.
- [53] W. I. F. David, K. Shankland, N. Shankland, *Chem. Commun.* **1998**, 931–932.
- [54] G. S. Pawley, *J. Appl. Crystallogr.* **1981**, *14*, 357–361.
- [55] A. R. Leach, *Molecular Modelling Principles and Applications*, Addison-Wesley Longman, Reading, MA, **1996**, pp. 2–4.

Received: March 4, 2003
Revised: June 24, 2003 [F4914]